Cooperative Control for Coordination Of UAVs Utilizing an Information Metric

William Selby

Abstract— **This research focuses on evaluating a cooperative control algorithm for multiple unmanned aerial vehicles (UAVs) as presented in [1]. This algorithm optimizes the amount of information acquired by a group of UAVs surveying several dispersed ground targets. The algorithm assumes the aerial vehicles are equipped with Ground Moving Target Indicators which estimate the target's bearing, range, and radial velocities. Simulated results of the algorithm are shown under different scenarios with varying initial conditions.**

I. INTRODUCTION

As the ability to control a single vehicle accurately and safely continues to develop, it is natural to progress to the ability to manage multiple vehicles. Groups of vehicles can be homogeneous or equipped with different sensor packages for various scenarios. Applications include resource allocation, target tracking, rendezvous, and distributed coverage of a specified area. These algorithms involve collecting information, distributing the information, and fusing the information to manipulate the vehicle group in a precise and beneficial way. As unmanned aerial vehicles become cheap and reliable platforms, it is clear that many cooperative control applications would involve these platforms.

This specific researches evaluates a cooperative control algorithm proposed in a series of papers by Bar-Shalom et al in [1], [2], and [3]. This algorithm assumes that each vehicle is equipped with a Ground Moving Target Indicator (GMTI). Multiple vehicles are used to track multiple ground targets. The Fisher information criterion is used to determine vehicle trajectories such that the total information obtained by the group of UAVs is maximized for the targets detected. The information criterion is computed as a function of detection probabilities of the targets, survival probabilities of the UAVs due to collisions with other UAVs, and hostile fire from the ground targets.The algorithm can work without prior knowledge of the targets, but for simulation purposes, global knowledge is assumed. The algorithm can also handle scenarios where new targets are detected. The communication requirements of this algorithm are low as well as the computational complexity. As an additional benefit, the distributed nature makes the algorithm robust to vehicle failure.

A. Related Work

Due to the wide variety of aerial platforms and their various applications, extensive research has been done in the area of cooperative control for coverage. One common approach to optimally place vehicles with respect to a bounded region is to place each vehicle at the center of a voronoi partition as shown in [4]. Specifically, Schwagger used voronoi partitions to position UAVs with downward facing cameras to optimally cover a desired area with the groups combined field of view [5]. As shown in Figure 1, this algorithm can be modified to provide optimal sensor coverage for target tracking as well. Voronoi partitions are also used for path planning in the face of known threats for UAVs trying to get near a target [6], [7], and [8].

As an alternative to the distance metric used for Voronoi partitions, some cooperative control algorithms compute the amount of information obtainable by the sensors at their given position. In [9], information gain is maximized for a decentralized network for management and control of multiple vehicles. In [10], the authors show that increasing the information value for individual or groups of vehicles acts as a cooperative control strategy. As the groups of vehicles, or flocks, get closer to

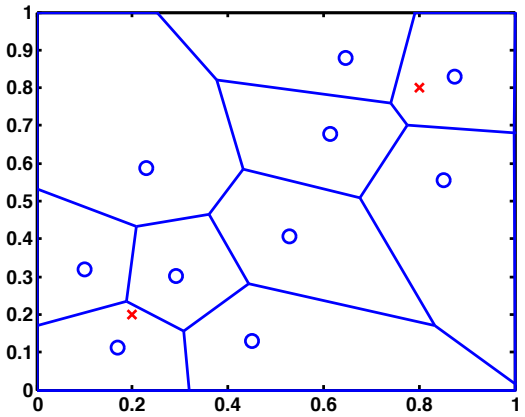

Fig. 1. Voronoi Partitioning for Coverage

the target, their information value increases. This causes the flocks merge, and the agents can perform cooperative filtering of their measurements using the distributed Kalman filtering algorithm. A thorough review of the use of the information value for decentralized data fusion can be found in [11]. Also, the determinant of the information matrix is evaluated in [12] to create a control algorithm that coordinates the motion of the vehicles to optimal positions for target tracking. Additional examples can be seen in [13] and [14].

II. Objective Function

The objective function, equation 1, is based on the Fisher information measurement which the authors explain in further detail in [3]. This approach is closely related to the problem of Decentralized Data Fusion (DDF). An advantage of an information measure is the ease of separating out what is new information from what is common or prior information. Since the process of combining information is additive as well as associative, the fusion process doesn't care which order the information came in. This is the main reason why this form of the Kalman filter is used for scalable and decentralized data fusion. It becomes possible to decentralize the process without worrying about when the information was communicated or combined [9].

$$J = \sum_j \log|(P_j(k|k)^{-1}| \tag{1}$$

where $P_j(k|k)^{-1}$ is the posterior covariance matrix of the state vector corresponding to target j at time k. $P_j(k|k)^{-1}$ is defined in terms of the state prediction covariance $P_j(k|k-1)$ and the new information $Y_j(k,s)$ that the UAVs can gather about the detected sensors as shown in 2.

$$P_j(k|k)^{-1} = P_j(k|k-1)^{-1} + \sum_s \pi_S(s)\pi_D(s,j)Y_j(k,s) \tag{2}$$

A. Survival Probability

The first term, $\pi_S(s)$, is the survival probability of UAV s which is computed as the product of target-fire survival probability $\pi_s^1(s)$ and the collision survival probability $\pi_s^2(s)$.

$$\pi_S(s) = \pi_s^1(s)\pi_s^2(s) \tag{3}$$

$\pi_s^1(s)$ is calculated as the product of the target-fire survival probabilities of UAV s in range of each target j.

$$\pi_s^1(s) = \prod_j \pi_s^1(s,j) \tag{4}$$

$\pi_s^1(s)$ is computed as the product of collision probabilities of UAV s and all other UAVs.

$$\pi_s^2(s) = \prod_{i,i\neq s} \pi_s^2(s,i) \tag{5}$$

B. Detection Probability

The second term in equation 2, $\pi_D(s,j)$, is the detection probability of target j by UAV s.

$$\pi_D(s,j) = \pi_D^1(s,i)\pi_D^2(s,i) \tag{6}$$

$\pi_D^1(s,i)$ is a simple function of the range between target j and vehicle s while $\pi_D^2(s,i)$ is a function of the range rate. The derivation of $\pi_D^2(s,i)$ is explained in equation 7. One specific

property of a GMTI radar is that they are unable to detect a target if the range rate of the target falls below a threshold $\dot{r}_{min}$.

$$\pi_D^2(s,i) = 1 - P\{-\dot{r}_{min} < \dot{r}(k,s,j) < \dot{r}_{min} | \dot{r}(k,s,j|k-1), \sigma_{\dot{r}}(k,s,j|k-1)^2\} \quad (7)$$

Here, $\dot{r}(k,s,j)$ is the measured range rate and $\dot{r}(k,s,j|k-1)$ is the predicted range rate given in equation 8

$$\dot{r}(k,s,j|k-1) = v_x^j(k|k-1)\text{cos}\alpha(k,s,j|k-1) + v_y^j(k|k-1)\text{sin}\alpha(k,s,j|k-1) \quad (8)$$

where $v_x^j(k|k-1)$ and $v_y^j(k|k-1)$ are components of the predicted velocity and the predicted azimuth for target j is $\alpha(k,s,j|k-1)$.

In equation 7, the variance term $\sigma_{\dot{r}}(k,s,j|k-1)^2$ is the range rate measurement prediction variance which is the third diagonal term of the innovation covariance matrix shown in equation 9.

$$S(k,s,j) = H(k,s,j)P_j(k|k-1)H(k,s,j)' = R(k,s,j) \quad (9)$$

In summary, the $\pi_D^2(s,i)$ term is computed by integrating a Gaussian density with mean $\dot{r}(k,s,j|k-1)$ and variance $\sigma_{\dot{r}}(k,s,j|k-1)^2$ over the interval $-\dot{r}_{min}$ to $\dot{r}_{min}$ and subtracting that probability from one.

The target-fire, collision survival, and detection probability functions are depicted in Figure 2. In real life, these are terrain dependent. This paper assumes the terrain is flat.

C. Information Matrix

The information matrix, $Y_j(k,s)$ characterizes the expected observation information gain of target j collected by UAV s calculated by equation 10.

$$Y(k,s,j) = H(k,s,j)'R(k,s,j)^{-1}H(k,s,j) \quad (10)$$

The state vector is shown in equation 11.

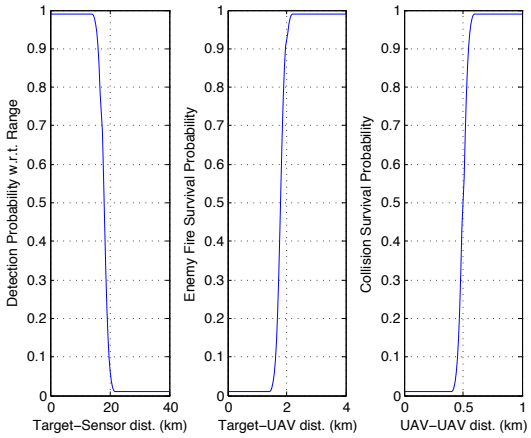

Fig. 2. Probability Functions

$$x = \begin{bmatrix} x^j & v_x^j & y^j & v_x^j \end{bmatrix}' \quad (11)$$

In the state vector, x and y are Cartesian coordinate positions and v_x and v_y are the velocity components. The measurement matrix is computed with equation 12.

$$H(k,s,j) = \begin{bmatrix} 1 & 0 & 0 & 0 \\ 0 & 0 & 1 & 0 \\ 0 & \text{cos}\alpha(k,s,j) & 0 & \text{sin}\alpha(k,s,j) \end{bmatrix} \quad (12)$$

The azimuth angle of target j measured by sensor s at time k is given by $\alpha(k,s,j)$. The measurements from the GMTI are azimuth $\alpha(k,s,j)$, range $r(k,s,j)$, and range rate $\dot{r}(k,s,j)$ which contain additive Gaussian noise with variances σ_α, σ_r, and $\sigma_{\dot{r}}$.

The measurement covariance matrix $R(k,s,j)$ is given in equation 13,

$$R(k,s,j) = \begin{bmatrix} R_{1,1} & R_{1,2} & 0 \\ R_{1,2} & R_{2,2} & 0 \\ 0 & 0 & \sigma_{\dot{r}}^2 \end{bmatrix} \quad (13)$$

where

$$R_{1,1} = r^2\sigma_\alpha^2 \text{sin}\alpha^2 + \sigma_r^2 \text{cos}\alpha^2 \tag{14}$$

$$R_{2,2} = r^2\sigma_\alpha^2 \text{cos}\alpha^2 + \sigma_r^2 \text{sin}\alpha^2 \tag{15}$$

$$R_{1,2} = (\sigma_r^2 - r^2\sigma_\alpha^2)\text{sin}\alpha\text{cos}\alpha \tag{16}$$

Lastly, the state covariance matrix $P_j(k|k-1)^{-1}$ is computed as shown in equation 17 for each target j. For the simulated results in this paper, the steady state value of $P_j(k|k-1)^{-1}$ was used as described in [2] and [3]. $P_j(k|k-1)^{-1}$ is calculated using the information filter form of the Riccati equation.

$$P_j(k|k-1)^{-1} = (A_j(k) + Q)^{-1} \tag{17}$$

$$A_j(k) = (F^{-1})'(P_j(k-1|k-1)^{-1} + Y(k))F^{-1} \tag{18}$$

Here, $\Delta_k = t_k - t_{k-1}$ and the transition matrix F is computed from equation 19.

$$F = \begin{bmatrix} 1 & \Delta_k & 0 & 0 \\ 0 & 1 & 0 & 0 \\ 0 & 0 & 1 & \Delta_k \\ 0 & 0 & 0 & 1 \end{bmatrix} \tag{19}$$

The process noise matrix follows a discrete white noise acceleration model with σ_v^2 as the variance of the white noise acceleration process.

$$Q = \begin{bmatrix} \frac{1}{4}\Delta_k^4 & \frac{1}{2}\Delta_k^3 & 0 & 0 \\ \frac{1}{2}\Delta_k^3 & \Delta_k^2 & 0 & 0 \\ 0 & 0 & \frac{1}{4}\Delta_k^4 & \frac{1}{2}\Delta_k^3 \\ 0 & 0 & \frac{1}{2}\Delta_k^3 & \Delta_k^2 \end{bmatrix} \sigma_v^2 \tag{20}$$

TABLE I

SIMULATION PARAMETER VALUES

Variable	Parameter	Value
T	Simulation time	100 sec
Δ_k	Timestep	1 sec
σ_α	Azimuth measurement variance	0.001 radians
σ_r	Range measurement variance	0.5 meters
$\sigma_{\dot{r}}$	Range rate measurement variance	0.1 m/s
σ_v	Noise acceleration variance	0.5 m/s^2

III. RESULTS

A. Static Scenario Simulated Results

Simulations were run using the values defined in Table I. The algorithm was simulated over several initial conditions. Each scenario had two UAVs and multiple targets. The first scenario had targets distributed around the vehicles. The second scenario had the targets aligned vertically.

In [3], the authors use a Newton-Raphson gradient descent algorithm to calculate the one step update for UAV position as defined in equation 21.

$$s_{new} = s_{old} - \beta(\bigtriangledown_s^2 J)^{-1} \bigtriangledown_s J \tag{21}$$

The Newton-Raphson method requires the first and second derivatives of the objective function with respect to x and y position of each UAV. This requires that the objective function be evaluated with the range and azimuth angles and then converted to derivatives with respect to the x and y position of the UAV. Instead, a simplified gradient descent method was chosen with respect to the dynamics of a quadrotor vehicle. The dynamics of the quadrotor allow it to hover as well as translate in any desired direction. A fixed wing UAV with nonholonomic constraints must maintain forward motion to generate lift.

For the following simulations, the vehicles were simulated forward in each of the cardinal directions and the objective function for these future positions was evaluated. The position which resulted in the largest reward value was chosen as the update. The UAVs moved at a constant speed of 3 m/s. This is summarized in equation 22 below.

$$\begin{aligned} \dot{x}(t) &= f(x(t), u(t)) \\ t &\in [t_0, t_f] \\ u^*(t) &= \arg\max_{u \in U} J(x(t), u(t)) \end{aligned} \tag{22}$$

Several steady state values of $P_j(k|k-1)^{-1}$ were used as explained in [2] and [3]. They are defined below.

$$P_1 = \begin{bmatrix} 10^2 & \frac{10}{3} & 0 & 0 \\ \frac{10}{3} & 1 & 0 & 0 \\ 0 & 0 & 10^2 & \frac{10}{3} \\ 0 & 0\frac{10}{3} & 1 & \end{bmatrix} \sigma_v^2 \tag{23}$$

$$P_2 = \begin{bmatrix} 500^2 & \frac{500}{3} & 0 & 0 \\ \frac{500}{3} & 5 & 0 & 0 \\ 0 & 0 & 500^2 & \frac{500}{3} \\ 0 & 0\frac{500}{3} & 5 & \end{bmatrix} \sigma_v^2 \tag{24}$$

$$P_3 = \begin{bmatrix} 500^2 & \frac{500}{3} & 0 & 0 \\ \frac{500}{3} & 5 & 0 & 0 \\ 0 & 0 & 10^2 & \frac{10}{3} \\ 0 & 0\frac{10}{3} & 1 & \end{bmatrix} \sigma_v^2 \tag{25}$$

When using P_1, the covariance values were relatively low. This resulted in the vehicles concentrating near the larger group of targets since this increases the amount of information obtainable. These results can be summarized by Figure 3 which depicts the reward as a function of time as well as the initial and final locations of the UAVs. The value of the reward increases as expected, since the goal is to maximize the Fisher information matrix. The spikes in the reward values are due to the additive Gaussian noise in the measurements of the GMTI sensors.

The second scenario has the targets placed in a vertical line with the UAVs starting on either side. Using the same steady state P_1 matrix, Figure 4 depicts the result of the algorithm with these initial conditions.

In this scenario, the optimal positions of the UAVs are on opposite sides of the targets in order to collect complimentary information from the targets.

When P_2 was used for the scenario with the targets dispersed around the UAVs, the following

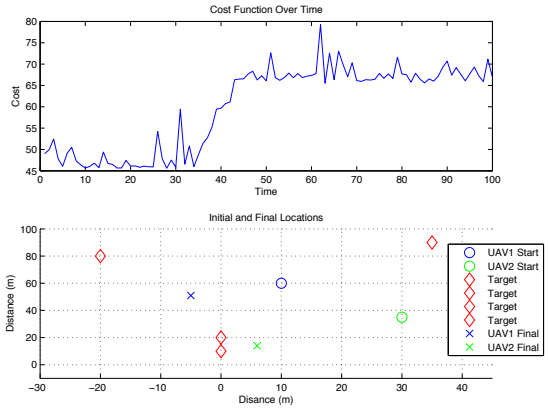

Fig. 3. Results Using Matrix P_1

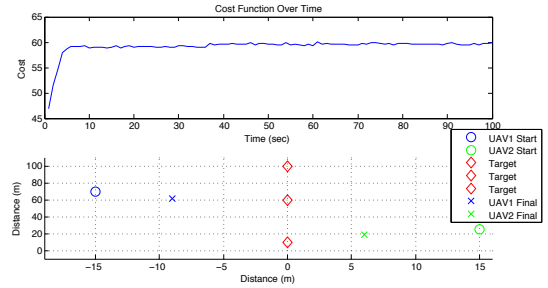

Fig. 4. Results Using Matrix P_1

results were obtained as shown in Figure 5. Since the covariances for the states are high, the quadrotors are forced to fill the space between the targets to gather as much information as possible.

When P_3 is used, the UAVs have a high covariance in the x axis but a low covariance in the y direction. This causes them to align themselves along the x axis in order to get better position and velocity information in this direction due to relatively less predicted information along this axis.

Distributed control has the distinct advantage of robustness to vehicle failures and additions. A scenario was considered using the initial conditions from Figure 6 where the targets are dispersed with the vehicles beginning between the targets. The effects of a potential third UAV was considered. Specifically, the algorithm was used to determine the optimal location to place the additional UAV

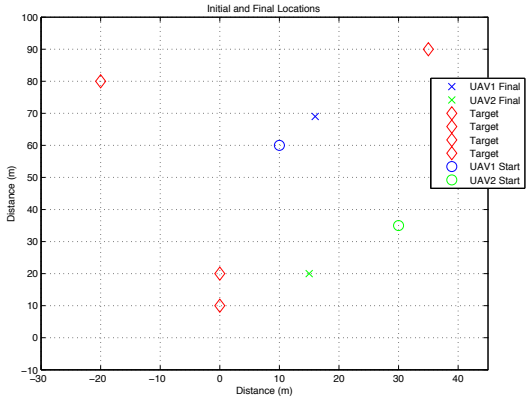

Fig. 5. Results Using Matrix P_2

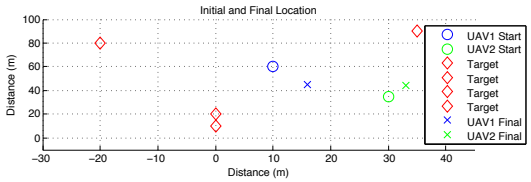

Fig. 6. Results Using Matrix P_3

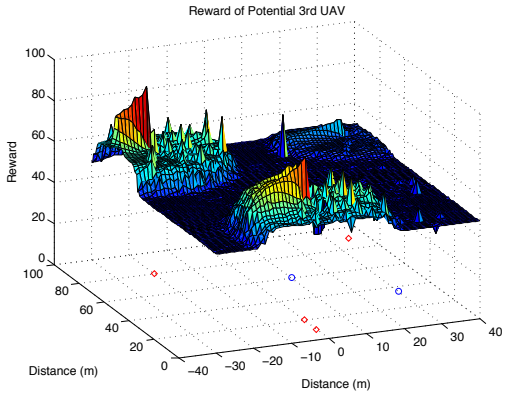

Fig. 7. Reward of Potential Third UAV

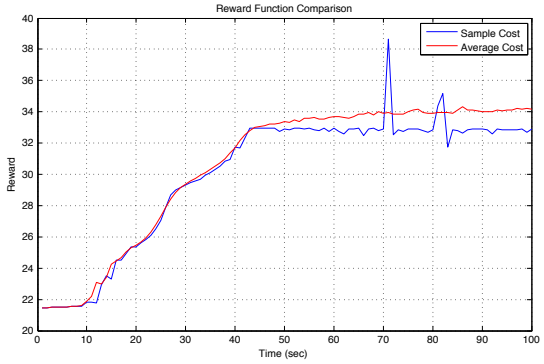

Fig. 8. Average Cost Function Over Time

if the others remained stationary. Figure 7 depicts the reward of the additional vehicle as its location is varied over the boundary using the steady state covariance matrix P_1. The locations of the current targets and vehicles are plotted below the surface. Analyzing this plot, it is evident that the additional vehicle should be placed near the cluster of targets or the target in the upper corner. The video attached with this report depicts the change of the potential reward surface over time as the two vehicles move in the environment.

Due to the noisy nature of the measurements and the discretization of the action space, the value of reward as a function of time function is not always a monotonically increasing function. In theory, the algorithm should always place the vehicles at a location with more reward than the previous position until the vehicles have reached a local maxima of the reward function. Figure 8 depicts the reward values for a single simulation compared to the average reward values of the same scenario simulated 50 times. While the single simulation resulted in a noisy reward value over time, the average reward values with respect to time appeared more true to the monotonically increasing form it should be. Increasing the number of simulations to average together would reduce this noise and show an aggregate behavior.

B. Dynamic Scenario Simulated Results

Lastly, this algorithm was extended to a scenario when only one UAV was available. Figure 9 depicts the evolution of a scenario where one UAV is tracking one target. The UAV immediately decreases the range to the target and follows behind the target as it moves. The reward as a function of time is also

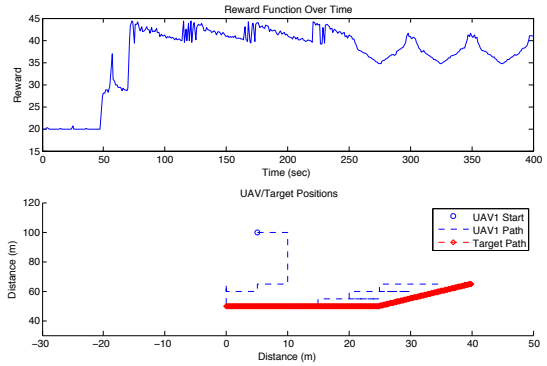

Fig. 9. Path of One UAV Tracking One Target

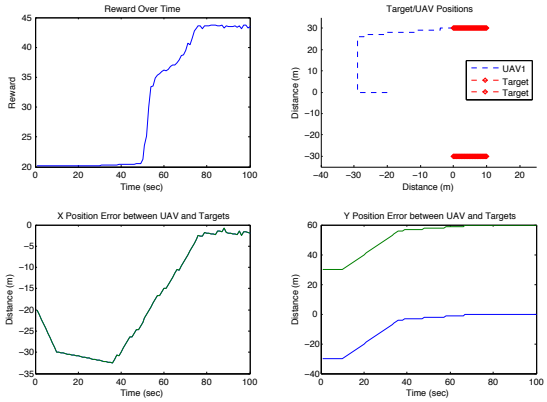

Fig. 10. Path of One UAV Tracking Two Targets

plotted.

Figure 10 depicts a single UAV tracking multiple targets. This could represent a scenario when the UAV is tracking multiple targets through a computer vision system. The targets could diverge and leave only one target in the field of view of the camera. In simulation, the algorithm causes the UAV to chose one target to follow. The UAV can get more information by remaining close to a single target rather than placing itself between the two targets. The target it choses is random due to the noise in the measurements if the vehicles are equidistant apart. If the UAV is closer to one target, it will chose that target to follow.

IV. CONCLUSIONS AND FUTURE WORKS

A. *Conclusions*

This research explored and alternative to voronoi partitioning as a means of cooperatively controlling a group of UAVs for coverage. Specifically, an algorithm based on maximizing the Fisher information metric as proposed by Bar-Shalom was evaluated and extended. Assuming the UAVs are equipped with GMTIs, the UAVs are placed to maximize the amount of information the UAVs can collect about the targets. This objective function was simulated with slight modifications. A simple double integrator model was used for the dynamics and a modified gradient descent approach was used to find relative maxima of the reward function. The effects of noise in the state prediction matrix was evaluated under several different scenarios. The algorithm was also extended to the case of a single UAV tracking a single and multiple targets to simulate a visual servoing scenario.

B. *Future Works*

In the future, the gradient of the objective function could be explicitly calculated using the proposed Netwon-Raphson method. This would decrease the noise seen in the reward function values over time and result in more accurate simulations. Simulating more dynamic UAVs and targets will also lead to a deeper understanding between the effects of noise in the system and the aggregate behavior of the UAV group. Lastly, this algorithm could be verified in hardware for simple scenarios to demonstrate the communication requirements and complexity of computations.

REFERENCES

[1] A. Sinha, T. Kirubarajan, and Y. Bar-Shalom, "Autonomous ground target tracking by multiple cooperative uavs," in *Aerospace Conference, 2005 IEEE*, March 2005, pp. 1 –9.

[2] A. Sinha, T. Kirubarajan, and Y. Bar-Shalom, "Optimal cooperative placement of UAVs for ground target tracking with Doppler radar," in *Society of Photo-Optical Instrumentation Engineers (SPIE) Conference Series*, ser. Presented at the Society of Photo-Optical Instrumentation Engineers (SPIE) Conference, I. Kadar, Ed., vol. 5429, Aug. 2004, pp. 95–104.

[3] A. Sinha, T. Kirubarajan, and Y. Bar-Shalomb, "Optimal cooperative placement of gmti uavs for ground target tracking," in *Aerospace Conference, 2004. Proceedings. 2004 IEEE*, vol. 3, March 2004, p. 1868 Vol.3.

[4] J. Cortes, S. Martinez, T. Karatas, and F. Bullo, "Coverage control for mobile sensing networks," in *Robotics and Automation, 2002. Proceedings. ICRA '02. IEEE International Conference on*, vol. 2, 2002, pp. 1327 –1332.

[5] M. Schwager, "A gradient optimization approach to adaptive multi-robot control," Ph.D. dissertation, Massachusetts Institute of Technology, United States of America, 2009.

[6] R. Beard, T. McLain, M. Goodrich, and E. Anderson, "Coordinated target assignment and intercept for unmanned air vehicles," *Robotics and Automation, IEEE Transactions on*, vol. 18, no. 6, pp. 911 – 922, Dec. 2002.

[7] S.-M. Li, J. Boskovic, S. Seereeram, R. Prasanth, J. Amin, R. Mehra, R. Beard, and T. McLain, "Autonomous hierarchical control of multiple unmanned combat air vehicles (ucavs)," in *American Control Conference, 2002. Proceedings of the 2002*, vol. 1, 2002, pp. 274 – 279 vol.1.

[8] T. W. McLain and R. W. Beard, "Trajectory planning for coordinated rendezvous of unmanned air vehicles," in *Proc. GNC2000*, 2000, pp. 1247–1254.

[9] J. Durrant-Whyte and B. Grocholsky, "Management and control in decentralised networks," in *Proceedings of International Conference on Information Fusion*, 2003, pp. 560–565.

[10] R. Olfati-Saber, "Distributed tracking for mobile sensor networks with information-driven mobility," in *American Control Conference, 2007. ACC '07*, July 2007, pp. 4606 –4612.

[11] B. Grocholsky, A. Makarenko, and H. Durrant-Whyte, "Information-theoretic coordinated control of multiple sensor platforms," in *Robotics and Automation, 2003. Proceedings. ICRA '03. IEEE International Conference on*, vol. 1, Sept. 2003, pp. 1521 – 1526 vol.1.

[12] S. Martnez and F. Bullo, "Optimal sensor placement and motion coordination for target tracking," *Automatica*, vol. 42, no. 4, pp. 661 – 668, 2006. [Online]. Available: http://www.sciencedirect.com/science/article/B6V21-4J8CXCB-3/2/60e6817efca3ea16f1f959fc6bd2599e

[13] F. Zhao, J. Shin, and J. Reich, "Information-driven dynamic sensor collaboration," *Signal Processing Magazine, IEEE*, vol. 19, no. 2, pp. 61 –72, March 2002.

[14] T. H. Chung, V. Gupta, J. W. Burdick, and R. M. Murray, "On a decentralized active sensing strategy using mobile sensor platforms in a network," in *in 43rd IEEE Conference on Decision and Control*, 2004, pp. 1914–1919.